On the texture in diffusion-grown layers of silicides and germanides with the FeB structure, MeX (Me = Ti,Zr; X = Si,Ge) or the ZrSi2 structure (ZrSi2, HfSi2, ZrGe2)

J. Appl. Cryst. (1984). **17**, 103–110

On the Texture in Diffusion-Grown Layers of Silicides and Germanides with the FeB Structure, MeX (Me = Ti, Zr; X = Si, Ge) or the $ZrSi_2$ Structure ($ZrSi_2$, $HfSi_2$, $ZrGe_2$)

BY J. H. MAAS,* G. F. BASTIN, F. J. J. VAN LOO AND R. METSELAAR

Laboratory for Physical Chemistry, Eindhoven University of Technology, PO Box 513, 5600 MB Eindhoven, The Netherlands

(*Received* 27 *June* 1983; *accepted* 5 *December* 1983)

Abstract

In diffusion-grown layers of compounds with the orthorhombic FeB- and $ZrSi_2$-type structures a pronounced texture is present which is rotationally symmetric with respect to the direction of diffusion. In FeB-type structures a [101]-fibre texture is observed for ZrSi and HfSi and a [100]-fan texture for TiSi and ZrGe. In $ZrSi_2$-type compounds the b axis is always perpendicular to the direction of diffusion; different compounds, however, show different textures: a [010]-fan texture for $ZrSi_2$, a [100]-fibre texture for $HfSi_2$ and a ⟨101⟩-fibre texture for $ZrGe_2$. The textures are explained in terms of preferential diffusion along specific crystallographic directions which can be derived from the crystal structures. At high temperatures a second texture component has been observed in HfSi layers and in layers with the $ZrSi_2$ structure. This second component can be considered as a recrystallization texture and can be derived from the original texture by a rotation of the crystallites of 20–25° around a simple crystallographic direction. The existence of a so-called TiGe phase with the FeB structure in the temperature region 1070–1270 K is questionable. Only Ti_6Ge_5 has been produced and this compound showed a [001]-fibre texture.

Introduction

When intermetallic compounds are grown in the form of diffusion layers the crystallites very often show a preferential orientation. Such is the case, for instance, in many coatings grown on metal substrates. Several mechanisms may be responsible for the occurrence of such textures, including anisotropic diffusion (growth textures), annealing (recrystallization textures) and stresses in the layer (deformation textures). Often different mechanisms are active in the course of the layer formation and as a result several texture components may be present. We have undertaken a systematic study of the occurrence of texture in diffusion-grown layers. To obtain more insight in the importance of the diffusion mechanism for the development of preferred orientations we have chosen groups of isostructural compounds. In an earlier paper (Maas, Bastin, van Loo & Metselaar, 1983) we investigated phases with the $TiAl_3$ structure and related structures. In this paper we report our results for compounds with the FeB structure type, and the related $ZrSi_2$ structure.

The compound FeB has an orthorhombic crystal structure with chains of B atoms along the [010] direction (Schubert, 1964) (Fig. 1). Diffusion of B atoms takes place preferentially along these chains, resulting in highly anisotropic diffusion (Kunst & Schaaber, 1967). According to Kunst (1969), using a model of Heumann & Dittrich (1959), nuclei with the b axis parallel to the growth direction have the best chance for further growth. This results in the formation of a layer with columnar grains oriented more or less parallel to the direction of diffusion.

In view of the existence of this worked-out model it seemed especially interesting to investigate other binary compounds with the same structure. We have also investigated a few compounds which have some relationship with the first group, *viz* compounds with the $ZrSi_2$ structure. Analogous to the FeB structure we can discern chains of Si atoms, in this case parallel to the [001] direction.

Experimental procedures

The layers were formed in diffusion couples, using the pure metals as starting materials. Sandwich couples X–Me–X were heated in a vacuum furnace ($P < 1$ mPa) under an external load of 1 MPa at 1133 K. Generally, two layers were formed under these conditions, MeX_2 and MeX, MeX having the smallest layer thickness. In many cases the MeX_2 layer thus obtained was used again in a diffusion couple MeX_2–Me at higher temperatures.

After the formation of the diffusion layers the couples were ground and polished parallel to the diffusion direction for optical microscopy and perpendicular to the diffusion direction for X-ray measurements. For

*Present address: HTS/SVL, Sloetsweg 155, 7556 HM Hengelo (0), The Netherlands.

0021–8898/84/020103-08$01.50

this latter investigation the layers used were always at least 10 μm thick.

Texture diagrams of the diffusion layers were measured with a Philips texture goniometer, PW 1078, using Fe $K\alpha$ radiation. The measured intensities were corrected for defocusing effects at increasing tilt angles, with the aid of correction curves obtained on textureless samples. During the measurement the sample is rotated around two different angles for a given Bragg angle. One rotation takes place around an axis perpendicular to the sample surface (rotation angle α). The other rotation is performed around the line of intersection between the specimen surface and the plane constituted by the incident X-ray beam and the diffracted beam. The tilt angle with respect to the surface normal is the angle χ. To obtain the contribution of a given texture component we measure the corrected intensity $I(\chi,\alpha)$ for a reflection *hkl* with respect to the 'random intensity' $\bar{I}$. The random intensity is given by

$$\bar{I}=\frac{1}{2\pi}\int_0^{2\pi}\int_0^{\pi/2} I(\chi,\alpha)\sin\chi\,d\alpha\,d\chi. \qquad (1)$$

In the present investigation the texture was in all cases rotationally symmetric with respect to the direction of diffusion. In that case (1) reduces to

$$\bar{I}=\int_0^{\pi/2} I(\chi)\sin\chi\,d\chi. \qquad (2)$$

The tabulated χ values represent the angle of maximum intensity for a given reflection *hkl*. The texture sharpness f is defined by $f=I(\chi=0)/\bar{I}$, with $I(\chi=0)$ being the intensity of a reflection by a plane perpendicular to the fibre axis. If $f(\chi)$ is plotted against χ a more or less Gaussian shaped curve is obtained. In this paper the width at half-maximum height of this curve, $\Delta\chi(\frac{1}{2})$, is used as a measure of the texture sharpness.

Experimental results for compounds with the FeB structure

Introduction

The FeB structure is shown in Fig. 1. The structure shows a zigzag chain of B atoms in the [010] direction, characterized by the parameters A and λ. Table 1 gives a survey of the compounds with FeB structure investigated here, together with the relevant structural data. In this section the experimental results for these binary compounds will be presented.

The compound TiSi

In diffusion couples Ti–Si three layers are observed. Fig. 2 shows a photomicrograph of a couple heated at 1153 K for 300 h. The main layers are $TiSi_2$ and TiSi.

Table 1. *Compounds with the* FeB *structure*

Compound	Lattice constants (Å)	Chain parameters* (Å) A	λ
FeB	$a=5{\cdot}506$ $b=2{\cdot}952$ $c=4{\cdot}061$	1·80	1·03
TiSi	$a=6{\cdot}544$ $b=3{\cdot}638$ $c=4{\cdot}997$	2·17	1·19
ZrSi	$a=6{\cdot}995$ $b=3{\cdot}785$ $c=5{\cdot}296$	2·27	1·26
HfSi	$a=6{\cdot}855$ $b=3{\cdot}753$ $c=5{\cdot}191$	(2·26)	(1·26)
TiGe	$a=6{\cdot}834$ $b=3{\cdot}809$ $c=5{\cdot}223$	–	–
ZrGe	$a=7{\cdot}075$ $b=3{\cdot}904$ $c=5{\cdot}396$	(2·35)	(1·31)

*See Fig. 1(*c*) and text.

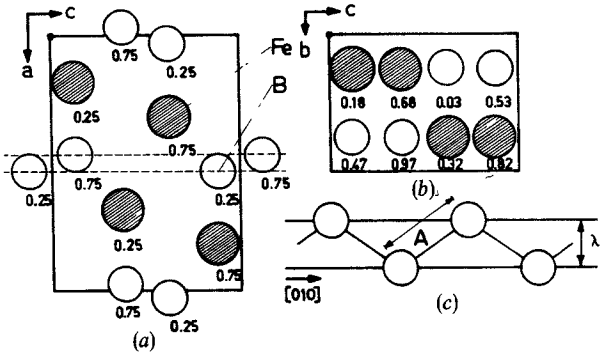

Fig. 1. FeB structure (Schubert, 1964), orthorhombic, D_{2h}^{16}, *Pnma*. (*a*) Projection on the (010) plane; (*b*) projection on the (100) plane; (*c*) zig-zag chain of B atoms in the [010] direction characterized by A and λ (*cf.* Table 1).

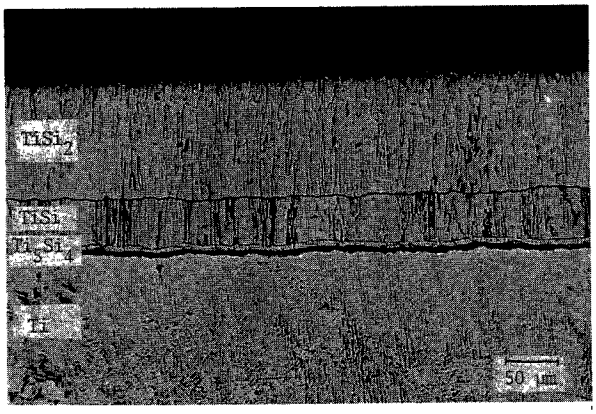

Fig. 2. Photomicrograph of a Ti–Si diffusion couple annealed for 308 h at 1153 K.

Table 2. *Results of texture measurements in* TiSi *layers*

Measured and calculated angles of the maxima with respect to the diffusion direction.

d_{hkl} (Å)	*hkl*	χ_{meas} (°) 1153 K	χ_{meas} (°) 1473 K	χ_{calc}* (°)
2·94	011	0	0	0·0
2·74	201	58	–	56·8
2·68	111	28	25	24·2
2·50	002	–	–	0·0
2·43	210	51	53	48·0
2·33	102	21	23	20·9
2·187	211	46	43	41·9
2·002	301	69	–	66·4
–	202	–	–	37·4
1·965	112†	19, 37	20, 37	17·5
		>65	>65	
1·820	020	0	0	0·0
1·752	311	55	–	53·4
1·555	401	72	–	71·9

*Angles calculated for a [100]-fan texture along the diffusion direction.

†Maxima at 37 and 65° are due to reflections 202 and 301, respectively, with overlapping Bragg angles.

We have also produced TiSi layers at 1473 K using $TiSi_2$/Ti couples.

After removal of the $TiSi_2$ layer by grinding, X-ray data were measured on the TiSi layer. The measured d_{hkl} values correspond closely with those calculated from the lattice parameters given in Table 1 (Schubert, 1964). An example of a texture diagram of five reflections is shown in Fig. 3. A survey of the results of texture measurements on TiSi layers produced at 1153 or 1473 K is shown in Table 2.

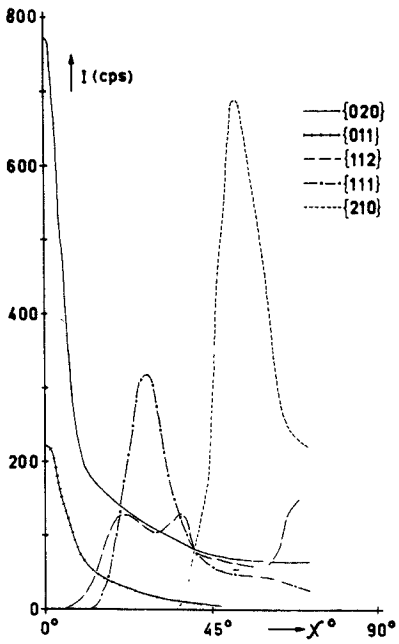

Fig. 3. Texture diagrams of five reflections *hkl* for TiSi grown at 1473 K.

Table 3. *Measured angles of the maxima with respect to the diffusion direction for* ZrSi *layers compared with angles calculated for a* [010]*-fibre texture*

d_{hkl} (Å)	*hkl*	χ_{meas} (°)	χ_{calc} (°)
3·07	011*	33	35·5
2·92	201	>70	90·0
2·57	210	47	47·3
2·47	102	>70	90·0
2·30	211	51	52·4
2·11	202	>70	90·0
2·07	112	54	56·8
1·88	020	0	0·0
1·66	220; 401	30	28·5; 90·0
1·589	221; 312	66	33·0; 65·2
1·499	122	37	37·4
1·415	321	39	41·6

*Rather diffuse maximum.

The reflection 002 is very weak, but is observed. The extra maxima at $\chi = 37$ and $\chi > 65°$ in the texture diagram of the 112 reflection are due to overlapping 202 and 301 reflections. From the intensity as a function of χ we observe a texture type which has been described by Huyser-Gerits, Rieck & Vogel (1970). The long axis of the columnar grains is parallel to the diffusion direction. The texture is described by a [100]-fibre axis perpendicular to the diffusion direction, a so-called [100]-fan texture. For comparison χ-values calculated for this texture are included in Table 2.

The texture is rather sharp, for instance the reflection 020 shows $\Delta\chi(\frac{1}{2}) = 8·5°$ for a layer grown at 1153 K. For layers grown at 1473 K the sharpness of this reflection even increases to 5·5°, without change in texture.

The compound ZrSi

In couples Zr–Si heated at 1153 K only $ZrSi_2$ and ZrSi layers are observed, with a thickness ratio of about 4:1. Fig. 4 shows a photomicrograph of such a couple. Results of texture measurements on ZrSi layers grown at 1153 K are given in Table 3. The

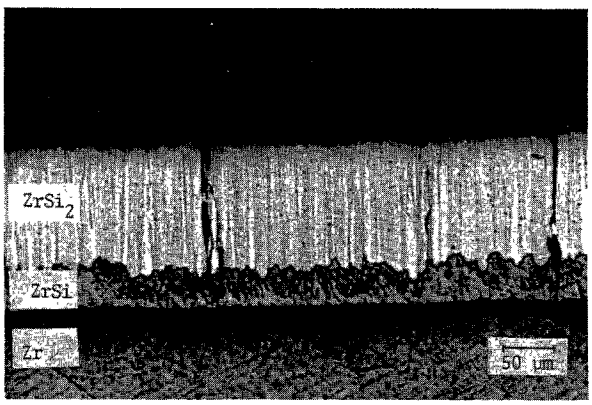

Fig. 4. Zr–Si diffusion couple annealed for 72 h at 1173 K.

measured d_{hkl} values agree with those calculated from the lattice parameters of Schubert (1964). The texture diagrams can be explained by the presence of a [010]-fibre texture parallel to the direction of diffusion. Values of χ calculated under this assumption are also shown in Table 3.

It has been attempted to obtain information on textures in ZrSi layers grown at higher temperatures, by using $ZrSi_2$–Zr couples. Interpretation of these measurements is hampered by evaporation of Zr and grain growth. Yet, it could be established that no other texture components develop at 1398 or 1523 K. The texture sharpness increases with increasing growth temperature as is evident from the $\Delta\chi(\frac{1}{2})$ values measured on the 020 reflection: $\Delta\chi(\frac{1}{2}) = 25°$ for layers grown at 1153 K, 19° for layers grown at 1398 K, and 12° for layers grown at 1523 K.

The compound HfSi

So far hardly any data have been published on diffusion in the Hf–Si system. Zmii, Seryugina, Kovtun & Kondratov (1973) report that $HfSi_2$ is formed from Hf and Si in the temperature range 1423–1473 K. At higher temperatures HfSi was also observed. In our experiments with diffusion couples of the type Hf–Si, at 1153 K, two layers were found, $HfSi_2$ and HfSi. At this temperature the HfSi layer is rather thin in comparison with the $HfSi_2$ layer. Suitable HfSi layers could also be produced in $HfSi_2$–Hf couples at 1523 K. An example is shown in Fig. 5. In this figure K denotes the Kirkendall plane, *i.e.* the original interface between the $HfSi_2$ and Hf layers. The position of the Kirkendall plane in the middle of the HfSi layer shows that Si is the only diffusing component. This follows from a consideration of the reaction equations $HfSi_2 \rightarrow HfSi + Si$ and $Hf + Si \rightarrow HfSi$.

Results of texture measurements on HfSi layers are shown in Table 4. In layers grown at 1523 K only a very sharp ⟨041⟩-fibre texture is observed, both near

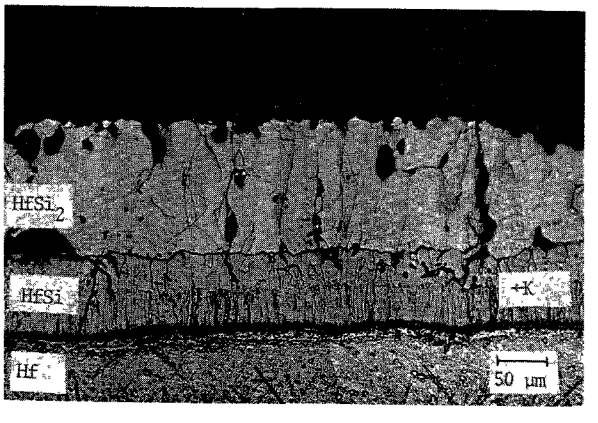

Fig. 5. Hf–$HfSi_2$ diffusion couple annealed for 24 h at 1523 K; K denotes the position of the Kirkendall interface.

Table 4. *Results for* HfSi

Positions of maxima in layers grown at 1153 or 1523 K, compared with positions calculated for a ⟨041⟩- or a [010]-fibre texture parallel to the diffusion direction.

d_{hkl} (Å)	hkl	χ_{meas} (°) 1153 K	χ_{meas} (°) 1523 K	χ_{calc} (°) ⟨041⟩	χ_{calc} (°) [010]
3·06	011	13; 36; 58	13; 55	16; 55	36
2·86	201	>70	>70	79	90
2·79	111	27; 43; 60	27; 59	28; 59	42
2·53	210	49	51	51	48
2·28	211		42; 66	44; 65	53
2·05	112	38; 57; 78	38; 77	39; 76	57
1·89	020	0; 21	21	20	0
1·72	121; 400		15; 44	14; 42; 90	24; 90
1·65	220; 401	31	36	34; 84	29; 90
1·49	122	18; 38; 59	18; 57	20; 56	38

the HfSi/$HfSi_2$ interface and the Hf/HfSi interface. This contrasts with the results in TiSi and ZrSi where only a [010] texture was found. However, in the thin HfSi layer formed at 1153 K the ⟨041⟩-texture component was observed together with a [010]-fibre texture. Table 4 also gives the calculated χ values for the two types of textures.

From the measured reflections we obtain lattice parameters which differ slightly from those given in Table 1 (Nowotny, Laube, Kieffer & Benesovsky, 1958). This work: $a = 6{\cdot}88$, $b = 3{\cdot}77$, $c = 5{\cdot}23$ Å.

The compound TiGe

In diffusion couples of the type Ge–Ti–Ge at 1153 K three layers are formed. The layers respectively bordering Ge and Ti, could be identified easily as $TiGe_2$ and Ti_5Ge_3 respectively. In accordance with the phase diagram (Elliott, 1965) the layer bordering $TiGe_2$ was expected to be TiGe. It was not possible, however, to give an interpretation of the texture measurements on the basis of data for TiGe (*cf.* Table 5). An excellent fit could be obtained between measured and calculated χ values if we assumed the layer to be Ti_6Ge_5 with a [001]-fibre texture.

Heating at 1153 or 1273 K of the diffusion couple Ti/$TiGe_2$ also gave the same result, *viz* Ti_6Ge_5 with a [001]-fibre texture. Finally, we tried to produce TiGe by argon arc melting. After annealing at 1173 K for 4 d two phases could be observed by optical microscopy. Powder diffraction experiments showed that a mixture of Ti_6Ge_5 and $TiGe_2$ was formed. Therefore, we doubt if TiGe is a stable compound near 1173 K. This doubt is strengthened by a consideration of the data plotted in Fig. 6. In this figure the cell volumes are plotted as a function of composition in the system Ti–Ge. The volume calculated from the data of Raman & Schubert (1965) for TiGe deviate strongly from the curve, while the volume calculated for Ti_6Ge_5 (Spinat, Fruchart & Herpin, 1970) fits well. For comparison the curve for the system Zr–Ge is also shown. Although Ti_6Ge_5 has a crystal structure which

Table 5. *Measured angles of maxima for the* 'TiGe' *layer in a* Ti–Ge *diffusion couple compared with calculated angles for a* [001]*-fibre texture parallel to the diffusion direction for the compounds* TiGe *and* Ti_6Ge_5

'TiGe'		TiGe			Ti_6Ge_5		
d_{hkl} (Å)	χ_{meas} (°)	d_{hkl} (Å)	*hkl*	χ_{calc} (°)	d_{hkl} (Å)	*hkl*	χ_{calc} (°)
3·60	>70	–	–	–	3.60	220	90
–	–	3·40	200	90	–	–	–
–	–	–	–	–	3·11	121, 510	53; 90
3·04	52	3·07	011	54	3·04	411	54
2·85	–	2·85	201	57	–	–	–
2·80	–	2·80	111	58	–	–	–
2·61	0	2·61	002	0	2·616	002	0
–	–	2·54	210	90	–	–	–
2·46	19	2·44	102	20	2·458	112	20
2·40	>70	–	–	–	2·399	330	90
2·37	60	–	–	–	2·370	611, 031	63
2·31	60	–	–	–	2·312	521, 710	64; 90
2·27	28; 62	2·28	211	64	2·275	312, 231	29; 64
2·22	30	–	–	–	2·223	402	32
2·18	33	–	–	–	2·187	022	33
1·94	40	–	–	–	1·941	422	42
1·90	65	1·90	020	90	1·903	811	69

differs considerably from the FeB structure, we mention here that a [001]-fibre texture was observed for this compound, with the fibre axis parallel to the diffusion direction.

The compound ZrGe

According to the phase diagram (Hansen & Anderko, 1958) four binary compounds can be formed between Zr and Ge: Zr_3Ge, Zr_5Ge_3, ZrGe and $ZrGe_2$. Rossteutscher & Schubert (1965) also observed the compound Zr_5Ge_4. In diffusion couples of the type Zr–Ge in the temperature range 1023–1153 K, $ZrGe_2$ is the only reaction layer. The adherence of this layer is bad, however, resulting in deformations of the couple. Also, cracks occur during cooling. Slightly better results were obtained when Ge + 1% *w/w* Zr was used instead of Ge. Fine needles of $ZrGe_2$ are formed, giving a better adherence.

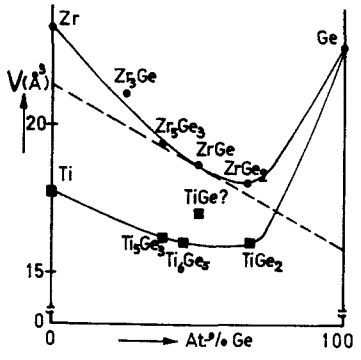

Fig. 6. Mean molar volume V as a function of composition in the binary systems Ti–Ge and Zr–Ge.

Table 6. *Angles of maxima measured in* ZrGe *layers compared with angles calculated for a* [100]*-fan texture or a* [010]*-fibre texture parallel to the diffusion direction*

d_{hkl}	*hkl*	$I/I^*_{0\,meas}$	χ_{meas} (°)	χ_{calc} (°) [100]-fan texture	χ_{calc} (°) [010]-fibre texture
3·16	011	*w*	–	0·0	35·9
2·88	111	*s*	32	24·1	42·3
2·70	002	*w*	–	0·0	90·0
2·62	210	*m*	49	47·8	47·8
2·52	102	*vs*	31	20·9	90·0
2·36	211	*w*	47	42·5	52·8
2·12	112	*vs*	28	17·4	57·1
1·95	020	*vs*	0	0·0	0·0
1·63	013	*w*	–	0·0	65·3
1·59	113	*w*	–	13·0	65·9
1·54	411	*s*	16	60·8	66·7
	122			12·6	37·8
1·35	004	*m*	–	0·0	90·0
1·16	132	*m*	–	9·4	27·3
1·11	024	*m*	–	0·0	55·4

*Relative intensity for the most important reflections with respect to the 210 reflection; mean value for six different layers.

Suitable ZrGe layers were obtained finally from diffusion couples Zr–$ZrGe_2$ after heating at 1273–1473 K in evacuated silica tubes. In these couples Zr_5Ge_4 is also observed as a reaction layer. A photomicrograph of a couple heated at 1293 K is shown in Fig. 7.

The results of texture measurements are summarized in Table 6. The reflection 020 always has a maximum intensity at $\chi = 0°$, *i.e.* parallel to the diffusion direction. Since the 210 reflection has a maximum at 49° a [100]-fan texture or a [010]-fibre texture can be present. The maxima of the 102 and 112 reflections lead us to the conclusion that a [100]-fan texture is present. This is also in accordance with the diffractogram. From the value $\Delta\chi(\frac{1}{2}) = 40°$ for the 020 reflection it follows that the texture is rather weak (compare with 6–9° for TiSi). In such a case deviations between measured and calculated values of χ are also possible.

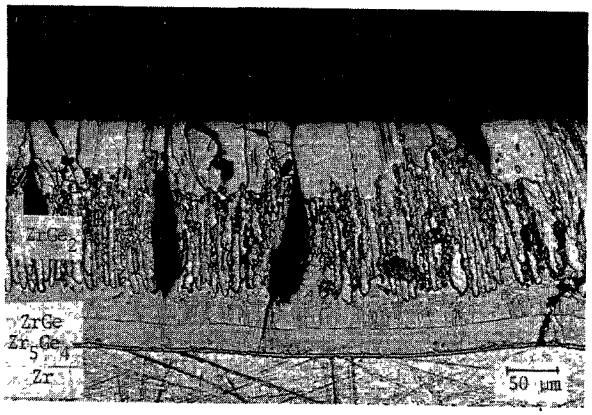

Fig. 7. Zr–$ZrGe_2$ diffusion couple annealed for 23 h at 1493 K.

Table 7. *Results of texture measurements for compounds with the* $ZrSi_2$ *structure*

	$ZrSi_2$	$HfSi_2$	$ZrGe_2$
Some important reflections	$a=3{\cdot}72$ Å $b=14{\cdot}69$ $c=3{\cdot}68$	$a=3{\cdot}677$ Å $b=14{\cdot}550$ $c=3{\cdot}649$	$a=3{\cdot}815$ Å $b=15{\cdot}090$ $c=3{\cdot}770$
hkl	χ_{meas} (°)	χ_{meas} (°)	χ_{meas} (°)
021	27	>80	51
130	38	38	51(Br)*
060	–	–	>80
131			
150	28; 52	50	31(Br); 63; >80
200	0	0	37(Br)
002	0	>80	47(Br)
202	0	45	0; >80
Texture type/ diffusion direction	[010]-fan texture	[100]-fibre texture	⟨101⟩-fibre texture

*(Br): peak broadened due to the presence of a second texture component.

Table 8. *Survey of the texture components observed in the* FeB*-type compounds investigated*

Compound	Temperature (K)	Texture components
TiSi	1153	[100]-fan texture
	1473	[100]-fan texture
ZrSi	1153	[010]-fibre texture
	1523	[010]-fibre texture
HfSi	1153	[010]- and ⟨041⟩-fibre texture
	1523	⟨041⟩-fibre texture
TiGe	1153	–*
	1273	–*
ZrGe	1293	[100]-fan texture
	1373	[100]-fan texture

*The compound TiGe with a FeB-type structure was not observed.

Experimental results for compounds with the $ZrSi_2$ structure

Three compounds were investigated: $ZrSi_2$, $ZrGe_2$ and $HfSi_2$. These compounds were always formed during the preparation of the corresponding compounds with FeB structure (Figs. 4, 5, 7). The layers of $ZrSi_2$ and $HfSi_2$ consist of fine needle-like crystallites with their axis parallel to the direction of diffusion. The results of X-ray measurements on these compounds are summarized in Table 7. The lattice parameters agree well with the data given by Schubert (1964). In all cases very sharp textures were observed. Also, in all cases, the texture sharpness decreased going from the metal/diffusion layer interface towards the interface Si(Ge)/diffusion layer. The [010] direction (*b* axis) of the crystallites is always perpendicular to the direction of diffusion.

Apart from the diffusion texture given in Table 7, a second texture component appeared upon annealing of the layers. The layers were grown at 1023–1173 K. During heating at 1273–1523 K the columnar structure disappeared and large approximately equiaxial crystallites appeared. At the same time a change in texture was observed. For $HfSi_2$ the [100]-fibre texture changed in a ⟨*uvw*⟩-fibre texture, approximately ⟨703⟩. This is interpreted as a tilt of the (100) plane of the crystallites around the [010] direction, over 24° with respect to the direction of diffusion. Also for $ZrSi_2$ and $ZrGe_2$ a similar tilt of the (100) plane around [010] over 20–25° was found. Owing to the increase in grain size the number of grains was in fact too small to determine the tilt angle with the same accuracy for the last two compounds mentioned.

Discussion

Table 8 gives a survey of the texture components observed in the FeB-type compounds. From this table we conclude that the crystallites always have their [100] direction perpendicular to the direction of diffusion. In TiSi and ZrGe no specific crystallographic direction in the (100) plane is parallel to the direction of diffusion, *i.e.* these compounds exhibit a [100]-fan texture. In ZrSi and HfSi (and also in FeB itself) the [010] direction in the (100) plane is parallel to the direction of diffusion, *i.e.* these compounds exhibit a [010]-fibre texture.

As mentioned already in the *Introduction*, Kunst & Schaaber (1967) and Kunst (1969) have proposed a model to explain the [010]-fibre texture in FeB. From the FeB structure, as shown in Fig. 1, it can be understood that B atoms diffuse preferentially in the [010] direction, since short B–B distances (1·80 Å) are found along the chains. For the compounds investigated, we also find that [010] chains are present with short distances between the Si (or Ge) atoms (~2·3 Å). The other interatomic distances are much larger (>3·7 Å). Other factors favouring this highly anisotropic diffusion are: the low steric hindering for atoms moving along the chains and the conservation of the ordering in the structure. Yet, only three of the five compounds (including FeB) show the expected [010]-fibre texture. In TiSi and ZrGe, with a fan texture, diffusion evidently does not take place along chains but in a plane, *viz* the (100) plane. A possible explanation may be sought in the highly anisotropic thermal expansion coefficients of these compounds. A maximum expansion occurs along the [100] direction, and the difference with the expansion in the [010] and [001] directions increases considerably with increasing temperature (Lyakhovich & Kosachevskii, 1973). This means that the vibration frequencies, and therefore also the jump frequencies in the (100) plane, increase relative to those perpendicular to this plane. A second reason for the change in texture may be sought in changes in relative atomic sizes as shown in

Fig. 8. The figure gives the ratio of the radius of the metal atom and the covalent radius of the non-metallic component. Also shown is the ratio of the radius of the metal atom and half the interatomic distance in the chain. Components with fan textures are on the left-hand side in this figure; however, the effect is not very pronounced.

For the compounds with $ZrSi_2$ structure the results have been summarized in Table 7. The crystal structure is shown in Fig. 9. In the FeB structure the metal atoms form columns consisting of triangular prisms parallel to the [010] direction. The B atoms are situated in the centre of these prisms. The building unit, a triangular prism of metal atoms containing a B (or Si, or Ge) atom is found in several structures, *e.g.* CrB-, MoB- and also $ZrSi_2$-type structures. In the $ZrSi_2$ structure the Si atoms form chains parallel to the [001] direction. In this structure we also find layers occupied only by Si atoms, parallel to the (010) plane.

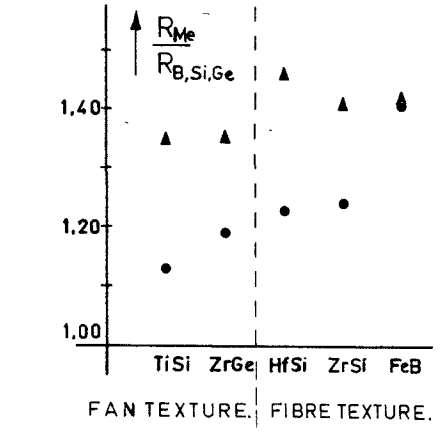

Fig. 8. Ratio of atomic radii in compounds with the FeB structure. ● $R_{metal}/R_{B,Si,Ge}$; ▲ $R_{metal}/\frac{1}{2}A$ (*cf.* Fig. 1*c*).

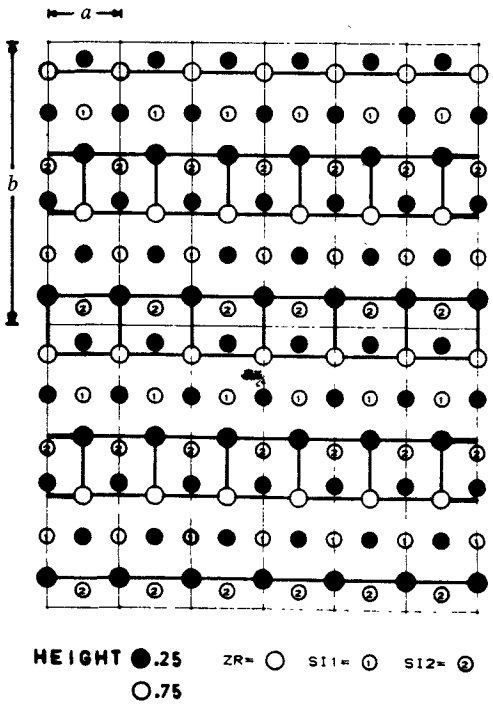

Fig. 9. $ZrSi_2$ crystal structure, projected on the (001) plane.

Table 9. *Survey of the relations observed between texture and structure for the different compounds investigated*

Structure type	Structural aspects	Texture types‖ diffusion direction
FeB	Chains of B atoms‖*b* axis	[010]-fibre texture (FeB, ZrSi, HfSi) [100]-fan texture (TiSi, ZrGe) ⟨041⟩-fibre texture (HfSi)
$ZrSi_2$	Layers of Si atoms ⊥ *b* axis	[010]-fan texture ($ZrSi_2$) [100]-fibre texture ($HfSi_2$) ⟨101⟩-fibre texture ($ZrGe_2$) ⟨*uvw*⟩-fibre texture* ($ZrSi_2$, $HfSi_2$ and $ZrGe_2$)
$NbCr_4Si_5$	Rows of Si atoms‖*c* axis	[001]-fibre texture (Ti_6Ge_5)

*The ⟨*uvw*⟩-fibre axis is obtained by a rotation around the *b* axis over 20–25° (compare with HfSi).

If diffusion along the chain occurs, as in the FeB structure, the crystallites in the $ZrSi_2$-type compounds would be expected to grow preferentially with the [001] direction parallel to the direction of diffusion. As can be seen from Table 7, none of the textures observed agrees with this model. This difference in behaviour for the FeB- and $ZrSi_2$-type structures is probably due to the differences in interatomic distances. For instance, in ZrSi the Si–Si distance in the chain is 2·27 Å, and considerably smaller than all other Si–Si distances (>3·80). In $ZrSi_2$ the Si–Si distance in the chain is larger, 2·43 Å according to Vaughan & Bracuti (1955) or 2·56 Å according to Schachner, Nowotny & Kudielka (1954), and nearly equal to the other Si–Si distances in the unit cell (2·62 Å).

According to our experiments the [010] direction is always perpendicular to the direction of diffusion. Evidently, there is a preference for diffusion in the Si layers occurring perpendicular to the *b* axis (*cf.* Fig. 9). The interatomic distances between the Si atoms is hardly different (2·62 Å) from that in the chain (~2·5 Å). It is not clear, however, why the diffusion occurs in $ZrSi_2$ in all directions perpendicular to

[010], in $HfSi_2$ only along [100] and in $ZrGe_2$ along ⟨101⟩. Referring to Table 9 we conclude that there is a relation between the type of texture and characteristic diffusion paths in the crystal structure. However, no choice can be made between diffusion in a plane or along a specific direction in that plane (fan or fibre texture).

A possible argument against the explanation given for the growth textures would be that grain-boundary diffusion may play a more important role than volume diffusion. However, in all experiments the same texture was observed both at low and high temperatures (apart from recrystallization, see below). Moreover, the texture sharpness increases at higher growth temperatures, where grain-boundary diffusion becomes less important.

Apart from the texture discussed above another texture component is possible, especially at higher temperatures. This second component is related to the first one by a rotation around a simple crystallographic direction. In Table 9 these texture components have been indicated separately (below the dashed lines). They are attributed to a recrystallization process, as is evident from the changes in morphology (change from fine needle-like to coarse equiaxial crystallites).

For completeness, we also mention the results obtained for Ti_6Ge_5. This compound has the layer structure of $Nb_2Cr_4Si_5$ (Kripyakevish, Yarmolyuk & Gladyshevskii, 1968), with close-packed layers at $z=0$ and $z=\frac{1}{2}$ alternating with scarcely occupied layers at $z=\frac{1}{4}$ and $z=\frac{3}{4}$. Important are the densely occupied rows of Ge atoms, with short interatomic distances, in the [001] direction. From these geometrical considerations preferential diffusion along [001] directions is to be expected. The texture observed is in accordance with this model.

In conclusion we can say that the textures observed for the FeB- and $ZrSi_2$-type compounds can be explained largely on the basis of a preferred diffusion direction, but that details cannot be explained with the models of Heumann and Kunst.

We are grateful to Professor G. D. Rieck who initiated this research and to Mr J. W. G. A. Vrolijk for his assistance in preparing computer drawings of crystal structures.

The investigations were supported by the Netherlands Foundation for Chemical Reseach (SON) with financial aid from the Netherlands Organization for the Advancement of Pure Research (ZWO).

References

ELLIOTT, R. P. (1965). *Constitution of Binary Alloys*, 1st Suppl. pp. 492–493. New York: McGraw Hill.

HANSEN, M. & ANDERKO, K. (1958). *Constitution of Binary Alloys*, pp. 780–781. New York: McGraw-Hill.

HEUMANN, TH. & DITTRICH, S. (1959). *Z. Metallkd.* **50**, 617–625.

HUYSER-GERITS, E. M. C., RIECK, G. D. & VOGEL, D. L. (1970). *J. Appl. Cryst.* **3**, 243–250.

KRIPYAKEVICH, P. I., YARMOLYUK, YA. P. & GLADYSHEVSKII, E. I. (1968). *Kristallografiya*, **13**, 781–786.

KUNST, H. (1969). *Texturen in Forschung und Praxis*, edited by J. GREWEN & G. WASSERMANN, pp. 375–381. Berlin: Springer.

KUNST, H. & SCHAABER, O. (1967). *Härterei-Techn. Mitt.* **22**, 1–25.

LYAKHOVICH, L. S. & KOSACHEVSKII, L. N. (1973). *Zashch. Pokriytiya Met.* **7**, 80.

MAAS, J. H., BASTIN, G. F., VAN LOO, F. J. J. & METSELAAR, R. (1983). *Z. Metallkd.* **74**, 294–299.

NOWOTNY, H., LAUBE, E., KIEFFER, R. & BENESOVKY, F. (1958). *Monatsh. Chem.* **89**, 701–707.

RAMAN, A. & SCHUBERT, K. (1965). *Z. Metallkd.* **56**, 40–43.

ROSSTEUTSCHER, W. & SCHUBERT, K. (1965). *Z. Metallkd.* **56**, 813–822.

SCHACHNER, H., NOWOTNY, H. & KUDIELKA, H. (1954). *Monatsh. Chem.* **85**, 1140–1153.

SCHUBERT, K. (1964). *Kristallstrukturen zweikomponentiger Phasen*. Berlin: Springer.

SPINAT, P., FRUCHART, R. & HERPIN, P. (1970). *Bull. Soc. Fr. Minéral. Cristallogr.* **93**, 23–36.

VAUGHAN, P. A. & BRACUTI, A. (1955). Abstr. Am. Crystallogr. Assoc. Summer Meet. p. 8.

ZMII, V. I., SERYUGINA, A. S., KOVTUN, N. V. & KONDRATOV, YU. T. (1973). *Inorg. Mater. (USSR)*, **9**, 707–709.